

Comparison of Isoelectronic 8-HO-G and 8-NH₂-G Derivatives in Redox Processes

Panagiotis Kaloudis,^{†,‡} Mila D'Angelantonio,[†] Maurizio Guerra,[†] Marie Spadafora,[†] Crina Cismaș,^{‡,§} Thanasis Gimisis,[‡] Quinto G. Mulazzani,[†] and Chrysostomos Chatgililoglu^{*,†}

ISOF, Consiglio Nazionale delle Ricerche, Via P. Gobetti 101, 40129 Bologna, Italy, and Department of Chemistry, University of Athens, 15771 Panepistimiopolis, Athens, Greece

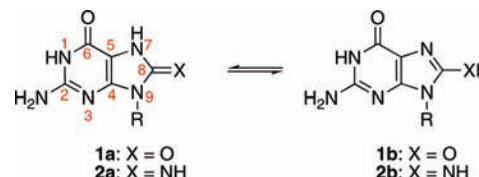
Received August 5, 2009; E-mail: chrys@isof.cnr.it

Abstract: 8-Oxo-7,8-dihydroguanine (8-oxo-G) is the major lesion of oxidatively generated DNA damage. Despite two decades of intense study, several fundamental properties remain to be defined. Its isoelectronic 8-aminoguanine (8-NH₂-G) has also received considerable attention from a biological point of view, although its chemistry involving redox processes remains to be discovered. We investigated the one-electron oxidation and one-electron reduction reactions of 8-oxo-G and 8-NH₂-G derivatives. The reactions of hydrated electrons (e_{aq}⁻) and azide radicals (N₃[•]) with both derivatives were studied by pulse radiolysis techniques, and the transient absorption spectra were assigned to specific tautomers computationally by means of time-dependent DFT (TD-B3LYP/6-311G**//B1B95/6-31+G**) calculations. The protonated electron adducts of 8-NH₂-G and 8-oxo-G showed a substantial difference in their absorption spectra, the unpaired electron being mainly delocalized in the imidazolyl ring and in the six-membered ring, respectively. On the other hand, the deprotonated forms of one-electron oxidation of 8-NH₂-G and 8-oxo-G showed quite similar spectral characteristics. In a parallel study, the one-electron reduction of 8-azidoguanine (8-N₃-G) afforded the same transient of one-electron oxidation of 8-NH₂-G, which represents another example of generation of one-electron oxidized guanine derivatives under reducing conditions. Moreover, the fate of transient species was investigated by radiolytic methods coupled with product studies and allowed self- and cross-termination rate constants associated with these reactions to be estimated.

Introduction

8-Oxo-7,8-dihydro-2'-deoxyguanosine (8-oxo-dGuo, **1**), an oxidation product of 2'-deoxyguanosine (dGuo), is commonly used as a biomarker of oxidative stress.^{1–4} This damage to the guanine moiety of DNA can be caused by hydroxyl radicals, singlet oxygen, or one-electron oxidants. Evidence that there are ~2000 8-oxo-G lesions generated per human cell per day has been reported.⁵ NMR studies⁶ and calculations⁷ have determined that the 6,8-diketo tautomer **1a** is the predominant species in solution with respect to the 8-hydroxy tautomer **1b** (Scheme 1). One-electron oxidation of 8-oxo-dGuo (as nucleo-

Scheme 1. Equilibrium of Two Tautomeric Forms of 8-Oxo-G (**1**) and of 8-NH₂-G (**2**)^{12 a}



^a The equilibrium is shifted to the left for **1** and to the right for **2** (in red, the atom numbering of guanine).

side⁸ or incorporated in oligonucleotides⁹) has been studied in some detail. Owing to its unique electronic properties,¹⁰ it has now been established that 8-oxo-dGuo is very susceptible to oxidation and far more reactive than dGuo itself toward one-electron oxidants and singlet oxygen.^{8,9} During the past 10 years a large number of studies appeared in the literature reporting the major and minor lesions formed from the oxidation of 8-oxo-dGuo analogues under a variety of oxidation conditions.^{1–4,11}

[†] Consiglio Nazionale delle Ricerche.

[‡] University of Athens.

[§] Present address: Organic Chemistry Department, Babes-Bolyai University, 11 Arany Janos str., 400028 Cluj-Napoca, Romania.

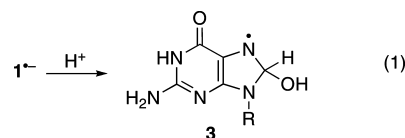
- (1) Gimisis, T.; Cismaș, C. *Eur. J. Org. Chem.* **2006**, 1351–1378.
- (2) Pratiel, G.; Meunier, B. *Chem.–Eur. J.* **2006**, *12*, 6018–6030.
- (3) Neeley, W. L.; Essigmann, J. M. *Chem. Res. Toxicol.* **2006**, *19*, 491–505.
- (4) Cadet, J.; Douki, T.; Ravanat, J.-L. *Acc. Chem. Res.* **2008**, *41*, 1075–1083.
- (5) (a) Beckman, K. B.; Ames, B. N. *J. Biol. Chem.* **1997**, *272*, 19633–19636. (b) Foksinski, M.; Rozalski, R.; Guz, J.; Ruszkowska, B.; Sztukowska, P.; Piwowarski, M.; Klungland, A.; Olinski, R. *Free Radical Biol. Med.* **2004**, *37*, 1449–1454.
- (6) Oda, Y.; Uesugi, S.; Ikehara, M.; Nishimura, S.; Kawase, Y.; Ishikawa, H.; Inoue, H.; Ohtsuka, E. *Nucleic Acids Res.* **1991**, *19*, 1407–1412.
- (7) Cysewski, P. *J. Chem. Soc., Faraday Trans.* **1998**, *94*, 3117–3125. Cysewski, P.; Jeziorek, D. *THEOCHEM* **1998**, *430*, 219–229.

- (8) Steenken, S.; Jovanovic, S. V.; Bietti, M.; Bernhard, K. *J. Am. Chem. Soc.* **2000**, *122*, 2373–2374.
- (9) Shafirovich, V.; Cadet, J.; Gasparutto, D.; Dourandin, A.; Huang, W.; Geacintov, N. E. *J. Phys. Chem. B* **2001**, *105*, 586–592.
- (10) Markus, T. Z.; Daube, S. S.; Naaman, R.; Fleming, A. M.; Muller, J. G.; Burrows, C. J. *J. Am. Chem. Soc.* **2009**, *131*, 89–95.
- (11) (a) Misiaszek, R.; Uvaydov, Y.; Crean, C.; Geacintov, N. E.; Shafirovich, V. *J. Biol. Chem.* **2005**, *280*, 6293–6300. (b) Munk, B. H.; Burrows, C. J.; Schlegel, H. B. *J. Am. Chem. Soc.* **2008**, *130*, 5245–5256.

8-Amino-2'-deoxyguanosine (8-NH₂-dGuo) and 8-aminoguanosine (8-NH₂-Guo, **2**) are produced together with the corresponding 8-oxo-guanine derivative, in rat liver treated with 2-nitropropane (2-NP), a hepatocarcinogen widely used as an industrial solvent, a component of coatings, and also found in cigarette smoke.^{13a} This has been shown to result from amination of DNA or RNA, respectively, by a metabolite of 2-NP, hydroxylamine-O-sulfonate, capable of releasing a reactive nitrenium ion (NH₂⁺).^{13b} Metal-mediated DNA damage caused by 2-NP metabolites may also play a role.¹⁴ This is a mutagenic lesion that has been found to generate G→T and G→C transversions in mammalian cells¹⁵ and to be weakly mutagenic (mutation frequency, 10⁻³) in *Escherichia coli*.¹⁶ To extenuate the difference between **1** and **2**, it was found that 8-NH₂-dGTP is incorporated and extended more efficiently than 8-oxo-dGTP by both HIV type I and murine leukemia virus reverse transcriptases and by DNA polymerases α and β.¹⁷ The analogous one-electron oxidation of 8-aminoguanine derivatives has not received any attention. The 8-NH₂-G moiety is also of particular interest, since it can be considered as a model compound of protein–DNA cross-links with the C8 position of the guanine moiety.^{18,19} NMR studies²⁰ and calculations²¹ suggest that the amino form **2b** rather than the imino **2a** form is the most stable tautomer in aqueous solutions, contrary to 8-oxo-G (Scheme 1).

Another interesting aspect related to 8-oxo-dGuo is the one-electron reduction process. Up to now this reaction has not received any attention. Nucleosides react with hydrated electrons (e_{aq}⁻) at practically diffusion-controlled rates to give radical anions. Radical anions of purine nucleosides, in particular, are rapidly protonated by water preferably at the C8 position, since the corresponding pK_a values are very high.²² For example, it has been recently reported that the guanine radical anion is protonated at C8.²³ 8-Bromoguanine derivatives are also protonated at C8 affording the corresponding one-electron oxidized guanine.^{24,25} If an analogous reaction applies to **1**, it can be expected to generate the HO• radical adduct **3** (Reaction 1), an

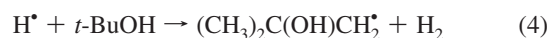
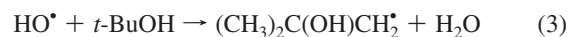
important intermediate for which spectroscopic and kinetic information is very scarce.²⁶



Herein we report detailed chemical radiation studies of compounds **1** and **2** in aqueous solution. In particular, we have investigated their one-electron oxidation and one-electron reduction reactions and clarified the major tautomeric forms of the various intermediates by the combined use of pulse radiolysis and DFT calculations. In addition, continuous radiolysis coupled with product studies allowed a better understanding of the fate of the transients.

Results and Discussion

Protonated One-Electron Reduced 8-Oxo-dGuo (1) and 8-NH₂-Guo (2) Species. Radiolysis of neutral water leads to e_{aq}⁻, HO•, and H• as shown in eq 2. The values in parentheses represent the radiation chemical yields (*G*) in units of μmol J⁻¹. The reactions of e_{aq}⁻ with the substrates were studied in O₂-free solutions containing 0.25 M *t*-BuOH. Based on the available kinetic data, we expected that HO• is scavenged efficiently (eq 3, *k*₃ = 6.0 × 10⁸ M⁻¹ s⁻¹), whereas H• is trapped only partially (eq 4, *k*₄ = 1.7 × 10⁵ M⁻¹ s⁻¹) under the utilized concentrations of *t*-BuOH.^{27,28}



The pseudo-first-order rate constants, *k*_{obs}, for the reaction of e_{aq}⁻ with 8-oxo-dGuo (**1**) and 8-NH₂-Guo (**2**) were determined by measuring the rate of the optical density decrease of e_{aq}⁻ at 720 nm ($\epsilon = 1.9 \times 10^4 \text{ M}^{-1} \text{ cm}^{-1}$)²⁹ at pH ~7. From the slope of *k*_{obs} vs nucleoside concentration, the bimolecular rate constants (*k*) of 5.6 × 10⁹ M⁻¹ s⁻¹ for **1** and 4.4 × 10⁹ M⁻¹ s⁻¹ for **2** are obtained. The optical absorption spectrum recorded at 2 μs after the pulse from the reaction of **1** (1.0 mM) with e_{aq}⁻ at natural pH (pH 7.2) is presented in Figure 1 (red circles) in the range 300–700 nm and shows a broad band that decreases at longer wavelengths. The time profile of the formation of this transient absorbance is identical to the disappearance of e_{aq}⁻, denoting a single process. The transient species decays with second-order kinetics, *k*/ε_{330 nm} = 8.2 × 10⁵ cm s⁻¹ (right inset). The optical absorption spectrum recorded at 2 μs after the pulse from the reaction of **2** (1.0 mM) with e_{aq}⁻ at natural pH (pH 8.1) is also presented in Figure 1 (blue triangles). The spectrum of this transient species is more intense than that obtained by the reaction of **1** with e_{aq}⁻, although its shape is only slightly different. This transient species decays with second-order kinetics, *k*/ε_{370 nm} = 1.8 × 10⁵ cm s⁻¹ (left inset), with a non-negligible plateau.

- (12) In schemes and figures, R = 2-deoxyribsyl for 8-oxo-G and R = ribosyl for 8-NH₂-G and 8-N₃-G. In the theoretical part (all tables) R = 2-deoxyribsyl.
- (13) (a) Fiala, E. S.; Nie, G.; Sodum, R.; Conaway, C. C.; Sohn, O. S. *Cancer Lett.* **1993**, *74*, 9–14. (b) Sodum, R. S.; Nie, G.; Fiala, E. S. *Chem. Res. Toxicol.* **1993**, *6*, 269–276.
- (14) Sakano, K.; Oikawa, S.; Murata, M.; Hiraku, Y.; Kojima, N.; Kawanishi, S. *Mutat. Res., Fundam. Mol. Mech. Mutagen.* **2001**, *479*, 101–111.
- (15) Tan, X.; Suzuki, N.; Johnson, F.; Grollman, A. P.; Shibutani, S. *Nucleic Acids Res.* **1999**, *27*, 2310–2314.
- (16) Venkatarangan, L.; Sivaprasad, A.; Johnson, F.; Basu, A. K. *Nucleic Acids Res.* **2001**, *29*, 1458–1463.
- (17) Kamath-Loeb, A. S.; Hizi, A.; Kasai, H.; Loeb, L. A. *J. Biol. Chem.* **1997**, *272*, 5892–5898.
- (18) Perrier, S.; Hau, J.; Gasparutto, D.; Cadet, J.; Favier, A.; Ravanat, J.-L. *J. Am. Chem. Soc.* **2006**, *128*, 5703–5710.
- (19) Xu, X.; Muller, J. G.; Ye, Y.; Burrows, C. J. *J. Am. Chem. Soc.* **2008**, *130*, 703–709.
- (20) Guengerich, F. P.; Mundkowski, R. G.; Voehler, M.; Kadlubar, F. F. *Chem. Res. Toxicol.* **1999**, *12*, 906–916.
- (21) Cysewski, P. *Z. Phys. Chem.* **2005**, *219*, 213–234.
- (22) Steenken, S. *Chem. Rev.* **1989**, *89*, 503–520.
- (23) D'Angelantonio, M.; Russo, M.; Kaloudis, P.; Mulazzani, Q. G.; Wardman, P.; Guerra, M.; Chatgililoglu, C. *J. Phys. Chem. B* **2009**, *113*, 2170–2176.
- (24) Chatgililoglu, C.; Caminal, C.; Guerra, M.; Mulazzani, Q. G. *Angew. Chem., Int. Ed.* **2005**, *44*, 6030–6032.
- (25) Chatgililoglu, C.; Caminal, C.; Altieri, A.; Mulazzani, Q. G.; Vougioukalakis, G. C.; Gimisis, T.; Guerra, M. *J. Am. Chem. Soc.* **2006**, *128*, 13796–13805.

- (26) Chatgililoglu, C.; D'Angelantonio, M.; Guerra, M.; Kaloudis, P.; Mulazzani, Q. G. *Angew. Chem., Int. Ed.* **2009**, *48*, 2214–2217.
- (27) Buxton, G. V.; Greenstock, C. L.; Helman, W. P.; Ross, A. B. *J. Phys. Chem. Ref. Data* **1988**, *17*, 513–886.
- (28) Ross, A. B.; Mallard, W. G.; Helman, W. P.; Buxton, G. V.; Huie, R. E.; Neta, P. *NDRLNIST Solution Kinetic Database - Ver. 3*, Notre Dame Radiation Laboratory, Notre Dame, IN and NIST Standard Reference Data, Gaithersburg, MD (1998).
- (29) Hug, G. L. *Nat. Stand. Ref. Data Ser., Nat. Bur. Stand.* **1981**, *69*, 6.

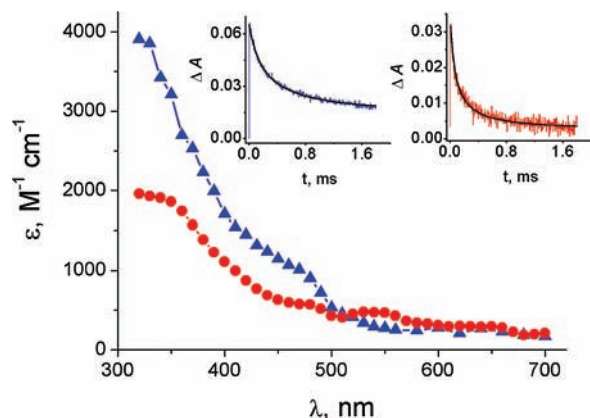


Figure 1. Absorption spectrum (red circles) obtained after pulse radiolysis at natural pH (pH 7.2) of 1.0 mM 8-oxo-dGuo (**1**), 0.25 M *t*-BuOH, Ar-purged, 2 μ s after the pulse. Absorption spectrum (blue triangles) obtained after pulse radiolysis at natural pH (pH 8.1) of 1.0 mM 8-NH₂-Guo (**2**), 0.25 M *t*-BuOH, Ar-purged, 2 μ s after the pulse. Insets: Time dependence of absorptions at 330 nm, the solid lines represent the second-order kinetic fit to the data; (right/red) optical path length of 2 cm, dose 27.8 Gy, $G(\mathbf{5}) = 0.33 \mu\text{mol J}^{-1}$, (left/blue) optical path 2 cm, dose 26.7 Gy, $G(\mathbf{7}) = 0.33 \mu\text{mol J}^{-1}$.

What is the structure of the observed intermediate in the case of 8-oxo-dGuo? The assignment is not straightforward. As discussed above the electron adducts should be rapidly protonated. The hydroxyl radical adduct **3** (Reaction 1) can be excluded because it is reported to undergo fast ring opening with a rate constant of $2 \times 10^5 \text{ s}^{-1}$,³⁰ whereas the recorded intermediate decays by second-order kinetics. Unfortunately an optical absorption spectrum of **3** is not available because only the minor path (ca. 17%) of the HO \cdot radical reaction with guanine affords radical **3**, the main reaction (65%) being the hydrogen abstraction from the NH₂ moiety.²⁶ However, DFT calculations predicted the following vertical transitions λ/nm (oscillator strength, *f*): 294 (0.157), 308 (0.010), 366 (0.029), and 433 (0.44).²⁶

Time-dependent DFT calculations (TD-B3LYP/6-311G(d,p)//B1B95/6-31+G(d,p)) were carried out to compute vertical optical transitions of other possible intermediates. Comparison with the experimental UV–visible spectrum could allow establishment of which tautomer of the protonated one-electron reduced 8-oxo-dGuo radical is responsible for the absorption spectrum recorded after pulse radiolysis, since this theoretical method was found by us to predict optical transitions in nucleosides with reliability.^{23–26,31,32} The computed optical transitions are reported in Table 1.

As can be seen in Table 1, the absorption spectrum displayed in Figure 1 is well reproduced by the optical transitions computed for tautomer **5**. DFT-TD calculations predict two main transitions of moderate intensity at 299 and 315 nm with a slightly weaker transition at 354 and two weak transitions at 433 and 647 nm in good accord with the experimental spectrum that presents a broad main band of moderate intensity between 300 and 400 nm with weak features above 430 nm. Also the computed spectrum of tautomer **4** presents two bands of moderate intensity in the 300–350 nm spectral region at 300 and 320 nm; however a strong peak is computed at 341 nm in evident contrast with the experimental spectrum. On the other hand, the computed spectrum for tautomer **6** is in complete disaccord with the experimental one, since it presents only one

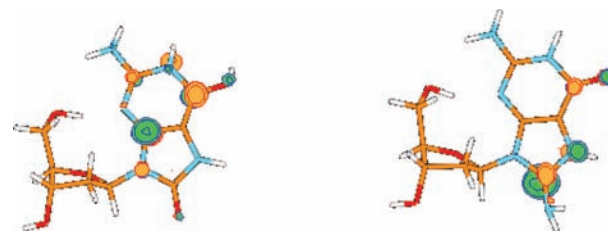


Figure 2. SOMO of the radicals **5** (left) and **7** (right) computed at the B3LYP/6-311G(d,p)//B1B95/6-31+G(d,p) level.

band of moderate intensity at a longer wavelength (349 nm). Interestingly, tautomer **5** is slightly more stable than tautomer **6** by 0.6 kcal mol⁻¹ at the PCM/B1B95/6-311+G(2df,p)//B1B95/6-31+G(d,p) level and more stable than tautomer **4** by 6.4 kcal mol⁻¹. This stability is due to the fact that in **5** the unpaired electron is delocalized in the six-member ring (Figure 2, left), whereas in **4** it is localized at C8.³³

In Figure 1 is shown that substitution of the oxy group with the amino/imino group at C8 produces an unexpected change in the absorption spectrum in that the intensity of the main band is twice as strong as that in the 8-oxo derivative. Furthermore, two shoulders are present at approximately 360 and 450 nm. This could be ascribed to different structures assumed by the two precursors. Indeed, DFT calculations at the PCM/B1B95/6-311+G(2df,p)//B1B95/6-31+G(d,p) level indicate that the amino **2b** form is more stable than the imino **2a** form by 4.8 kcal mol⁻¹, whereas the oxy **1a** form is more stable than the hydroxy **1b** form by 12.6 kcal mol⁻¹, in accord with NMR studies^{6,20} and the previous calculations.^{7,21} Then, DFT-TD calculations were carried out on the possible tautomers **7**, **8**, **9** deriving from protonation of the radical anion of **2b** at N7, O6', and N3 heteroatoms, respectively.

As revealed in Table 2, the computed spectrum for the N7–H tautomer **7** is in rather good accord with the experimental one. The main peak is computed to be due to overlap of two strong transitions at 313 and 331 nm; furthermore two shoulders are computed at 342 and 420 nm. On the other hand, the computed spectra for both tautomers **8** and **9** are in disaccord with the experimental one, since no band of moderate intensity is computed above 400 nm. In particular, only one band of moderate intensity is computed for **8** at 327 nm, and two bands of low intensity are computed for **9** in the 300–350 nm region. Interestingly, tautomer **7** is computed to be much more stable than both tautomers **8** (by 5.9 kcal mol⁻¹) and **9** (by 6.8 kcal mol⁻¹).

From Figure 2 (right), the SOMO of the radical **7** in which the unpaired electron is mainly delocalized in the imidazolyl ring can be seen, in contrast with radical **5** (left) where the unpaired electron is mainly delocalized in the six-membered ring.³³ These findings are in accord with experimental spectra recorded by pulse radiolysis upon one-electron reduction of 8-oxo-G (**1**) and 8-NH₂-G (**2**) derivatives, respectively.

To investigate in more detail the fate of the intermediate radicals, γ -radiolysis coupled with product studies was carried out. Deaerated samples containing either **1** (1.6 mM) and

(33) See Supporting Information.

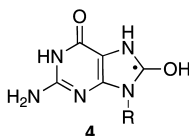
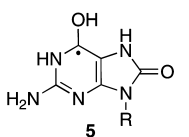
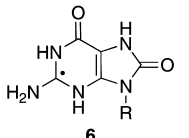
(34) The experiments of **1** (R = deoxyribosyl) in natural pH produce small amounts of free base (8-oxo-7,8-dihydro-guanine). It is known that radiolysis of neutral water, besides the transient species (eq 1), produces H⁺ in amounts that can alter the pH of the irradiated solution. In an independent experiment, the hydrolysis of **1**'s glycosidic bond was observed even in slightly acidic solutions. On the other hand, the increased stability of the glycosidic bond of the ribose moiety did not require buffered solutions as in the case of **2** (R = ribosyl).

(30) Candeias, L. P.; Steenken, S. *Chem.–Eur. J.* **2000**, *6*, 475–484.

(31) Chatgililoglu, C.; Guerra, M.; Mulazzani, Q. *G. J. Am. Chem. Soc.* **2003**, *125*, 3839–3848.

(32) Kaloudis, P.; D'Angelantonio, M.; Guerra, M.; Gimisis, T.; Mulazzani, Q. G.; Chatgililoglu, C. *J. Phys. Chem. B* **2008**, *112*, 5209–5217.

Table 1. Vertical Optical Transitions (Wavelengths λ , Oscillator Strengths f) for the Tautomers of Protonated One-Electron Reduced 8-Oxo-dGuo Computed at the TD-B3LYP/6-311G(d,p)//B1B95/6-31+G(d,p) Level^a

Tautomers	λ , nm	f	Transition {spin}
 4	300	0.040	SOMO($p\pi(C8)$) \rightarrow $\sigma^*(O8'-H)$ { α }
	320	0.028	$\pi(C4-C5) - p\pi(O6')$ \rightarrow $\pi^*(N1-C2) + \pi^*(C4-N9)$ { β }
	341	0.092	$\pi(C4-C5) - p\pi(O6')$ \rightarrow SOMO($p\pi(C8)$) { β }
	393	0.015	SOMO($p\pi(C8)$) \rightarrow $\pi^*(C2-N3) - \pi^*(C6-O6')$ { α }
	540	0.010	SOMO($p\pi(C8)$) \rightarrow $\pi^*(N1-C2) + \pi^*(C4-N9)$ { α }
 5	299	0.040	SOMO($p\pi(C4) - p\pi(C6)$) \rightarrow $\pi^*(C8-O8')$ { α }
	315	0.047	SOMO($p\pi(C4) - p\pi(C6)$) \rightarrow $p\pi(\text{out-of-phase } N3, C4, N9, C8, O8')$ { α }
	354	0.025	$\pi(C5-O6) - p\pi(N7) + p\pi(O8')$ \rightarrow SOMO($p\pi(C4) - p\pi(C6)$) { β }
	433	0.010	SOMO ($(p\pi(C4) - p\pi(C6))$) \rightarrow $\sigma^*(O6'-H)$ { α }
	647	0.016	SOMO($p\pi(C4) - p\pi(C6)$) \rightarrow $\pi^*(C2-N3) + \pi^*(C5-O6)$ { α }
 6	349	0.049	$\pi(C4-C5) + p\pi(O8')$ \rightarrow SOMO($p\pi(C2)$) { β }

^a Only transitions with f greater than, or equal to, 0.010 are reported.

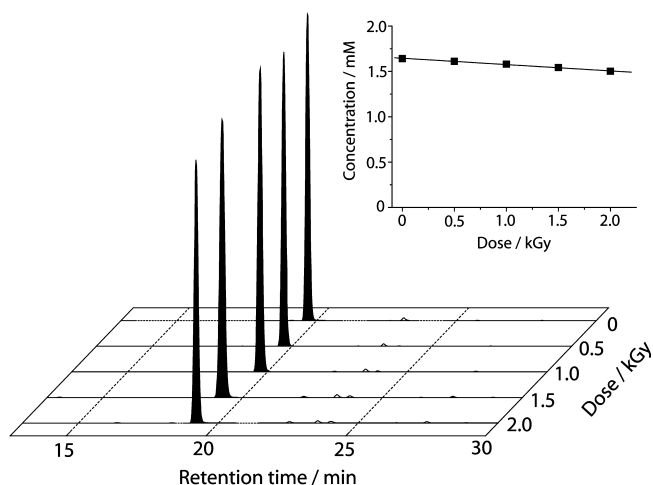
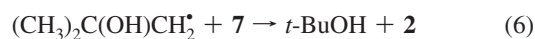
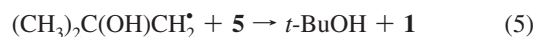


Figure 3. Irradiation of 1.6 mM 8-oxo-dGuo (**1**) in the presence of 0.25 M *t*-BuOH at pH = 7.0 (phosphate buffer) and at a dose rate of ~ 10 Gy min^{-1} . Inset: concentration of **1** vs dose.

t-BuOH (0.25 M) in phosphate buffered solution (pH = 7.0) or **2** (1.1 mM) and *t*-BuOH (0.25 M) at natural pH (pH 8.1) were irradiated under stationary state conditions with a dose rate of ca. 10 Gy min^{-1} followed by HPLC analysis.³⁴ Surprisingly, the only detectable product in both cases was the initial nucleoside, with a measurable loss of **1** or **2** of ca. 10% after 2

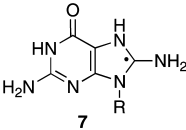
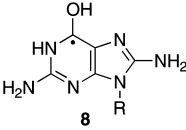
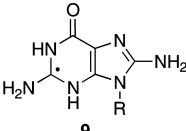
kGy, as illustrated in Figure 3 for 8-oxo-dGuo (see Supporting Information for 8-NH₂-Guo). Under our experimental conditions, a dose of 2 kGy generates ca. 0.66 mM radicals in the irradiated solution. Assuming that both e_{aq}^- and H^\bullet react with the substrates (cf. eq 2), a consumption of up to 41% or 60% would be expected for the starting nucleoside **1** or **2** after 2 kGy, in contrast with the experimental results.

Our mechanistic proposal to explain this unexpected finding involves a cross disproportionation reaction between the nucleosidic neutral radical and the $\text{}^{\bullet}\text{CH}_2\text{C}(\text{CH}_3)_2\text{OH}$ radical, which is formed after the reaction between HO^\bullet or H^\bullet and *t*-BuOH (eqs 5 and 6). As a result, both the starting nucleoside and *t*-BuOH are regenerated. This mechanism accounts for the lack of novel products in the irradiated solution, even after irradiation with high doses, as well as the low consumption of the starting nucleoside.



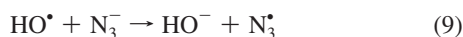
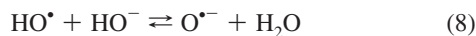
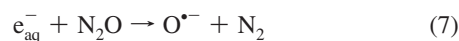
Taking into consideration that a rate constant of 6.0×10^8 $\text{M}^{-1} \text{s}^{-1}$ is reported for the radical–radical recombination of $(\text{CH}_3)_2\text{C}(\text{OH})\text{CH}_2^\bullet$ in aqueous solutions²⁸ and assuming a rate constant for self-termination of radicals **5** and **7** of 2.0×10^8 $\text{M}^{-1} \text{s}^{-1}$, it was possible to fit very well the decays of transients in Figure 1 (insets) using rate constants of 1.4×10^9 and 3.0×10^8 $\text{M}^{-1} \text{s}^{-1}$ for eqs 5 and 6, respectively.³³

Table 2. Vertical Optical Transitions (Wavelengths λ , Oscillator Strengths f) for the Tautomers of Protonated One-Electron Reduced 8-NH₂-dGuo Computed at the TD-B3LYP/6-311G(d,p)//B1B95/6-31+G(d,p) Level^a

Tautomers	λ , nm	f	Transition {spin}
 7	313	0.047	$\pi(\text{C4-C5}) - p\pi(\text{O6}') \rightarrow \pi^*(\text{N1-C2}) + \pi^*(\text{C4-N9})$ { β }
	331	0.063	$\pi(\text{C4-C5}) - p\pi(\text{O6}') \rightarrow \text{SOMO}(p\pi(\text{C8}))$ { β }
	342	0.032	$\text{SOMO}(p\pi(\text{C8})) \rightarrow \sigma^*(\text{N8'-H})$ { α }
	420	0.022	$\text{SOMO}(p\pi(\text{C8})) \rightarrow \pi^*(\text{C2-N3}) - \pi^*(\text{C6-O6'})$ { α }
	591	0.011	$\text{SOMO}(p\pi(\text{C8})) \rightarrow \pi^*(\text{N1-C2}) + \pi^*(\text{C4-N9})$ { α }
 8	288	0.011	$\text{SOMO}(p\pi(\text{C6})) \rightarrow \sigma^*(\text{N2'-H})$ { α }
	327	0.051	$\pi(\text{C4-C5}) - \pi(\text{N7-C8}) \rightarrow \text{SOMO}(p\pi(\text{C6}))$ { β }
 9	316	0.027	$\pi(\text{C4-C5}) - \pi(\text{N7-C8}) + p\pi(\text{N8'}) \rightarrow \text{SOMO}(p\pi(\text{C2}))$ { β }
	364	0.027	$\text{SOMO}(p\pi(\text{C2})) \rightarrow \pi^*(\text{N7-C8})$ { α }

^a Only transitions with f greater than 0.010 are reported.

Deprotonated One-Electron Oxidized 8-Oxo-dGuo (1) and 8-NH₂-Guo (2) Species. In the presence of N₂O, e_{aq}⁻ are efficiently transformed into the O^{•-} radical (eq 7, $k_7 = 9.1 \times 10^9 \text{ M}^{-1} \text{ s}^{-1}$).^{27,28} The HO[•] radical [$pK_a(\text{HO}^\bullet) = 11.9$] is in equilibrium with its conjugated base O^{•-} (eq 8, $k_8 = 1.2 \times 10^{10} \text{ M}^{-1} \text{ s}^{-1}$, $k_{-8} = 1 \times 10^8 \text{ s}^{-1}$).²⁷ The irradiation of N₂O-saturated solutions containing 0.1 M NaN₃ at pH \sim 7 causes the formation of the azide radical through the process shown in eq 9 ($k_9 = 1.2 \times 10^{10} \text{ M}^{-1} \text{ s}^{-1}$).^{27,28}



The optical absorption spectrum of the one-electron oxidized 8-oxo-dGuo (**1**) obtained by reaction of N₃[•] with **1** has been previously reported by Steenken and co-workers.⁸ Figure 4 shows this spectrum (black line) in the 300–700 nm range which consists of a sharp band centered at 320 nm and a broader band at 400 nm, assigned by Steenken to radical **10** or/and its tautomeric form **11**. The analogous reaction of N₃[•] with 8-NH₂-Guo (**2**) afforded a transient species that in the 320–700 nm range resembles the deprotonated one-electron oxidized 8-oxo-dGuo species (Figure 4, red circles). By measuring the rate of the optical density increase at 320 nm at different 8-NH₂-Guo concentrations, a rate constant of $3.5 \times 10^9 \text{ M}^{-1} \text{ s}^{-1}$ is obtained for the oxidation of **2** by N₃[•].³³ In analogy with 8-oxo-dGuo, we assign this transient to radical **12** or/and its tautomeric form **13** (Scheme 2).

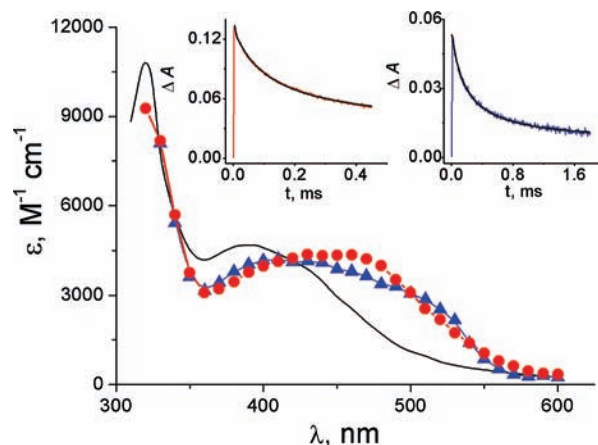


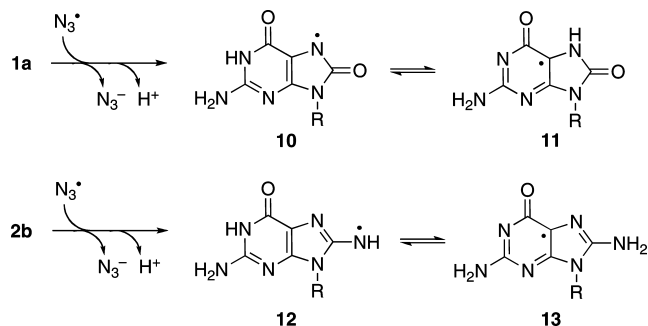
Figure 4. Absorption spectrum (black line) of one-electron oxidized 8-oxo-dGuo (**1**) taken from ref 8. Absorption spectrum (red circles) obtained after pulse radiolysis at natural pH (pH 8.1) of 1.0 mM 8-NH₂-Guo (**2**), 0.1 M NaN₃, N₂O-saturated, 2 μs after the pulse. Absorption spectrum (blue triangles) obtained after pulse radiolysis at natural pH of 1.0 mM 8-N₃-Guo (**16**), 0.25 M *t*-BuOH, Ar-purged, 2 μs after the pulse. Insets: Time dependence of absorption at 420 nm; the solid lines represent the second-order kinetic fit to the data; (left/red) optical path 2 cm, dose 28.2 Gy, $G(\mathbf{12}) = 0.61 \mu\text{mol J}^{-1}$, (right/blue) optical path 2 cm, dose 26.2 Gy, $G(\mathbf{12}) = 0.27 \mu\text{mol J}^{-1}$.

Time-dependent DFT calculations (TD-B3LYP/6-311G(d,p)//B1B95/6-31+G(d,p)) were carried out to compute vertical optical transitions of two tautomers **10** and **11** and to compare with the experimental UV–visible spectra. The optical absorption spectrum of the one-electron oxidized 8-oxo-dGuo displayed in Figure 4 is well reproduced by the optical transitions computed for tautomer **10** (Table 3). DFT-TD calculations predict one strong absorption at 296 nm that is in accord with

Table 3. Vertical Optical Transitions (Wavelengths λ , Oscillator Strengths f) for the Tautomers of Deprotonated One-Electron Oxidized 8-Oxo-dGuo Computed at the TD-B3LYP/6-311G(d,p)//B1B95/6-31+G(d,p) Level^a

Tautomers	λ , nm	f	Transition {spin}
10	296	0.234	SOMO($p\pi(N7) - p\pi(O8')$) $\rightarrow \pi^*(C2-N3) - \pi^*(C6-O6')$ { α }
	362	0.031	SOMO($p\pi(N7) - p\pi(O8')$) $\rightarrow \pi^*(N1-C2) + \pi^*(C4-N9)$ { α }
	382	0.045	$p\pi(\text{out-of-phase } N2', N1, (O6')) \rightarrow \text{SOMO}(p\pi(N7) - p\pi(O8'))$ { β }
11	300	0.017	$p\pi(N7) - p\pi(N9) - p\pi(O6') \rightarrow \text{SOMO}(p\pi(C5))$ { β }
	316	0.018	$p\pi(N7) \rightarrow \text{SOMO}(p\pi(C5))$ { β }
	443	0.044	$p\pi(\text{out-of-phase } N2', N3, N9, O8') \rightarrow \text{SOMO}(p\pi(C5))$ { β }
	496	0.013	$p\pi(\text{out-of-phase } N2', N3, N9, O8') \rightarrow \text{SOMO}(p\pi(C5))$ { β }
	703	0.010	$p\pi(\text{out-of-phase } N2', N1, O6') \rightarrow \text{SOMO}(p\pi(C5))$ { β }

^a Only transitions with f greater than 0.010 are reported.

Scheme 2. One-Electron Oxidation of 8-Oxo-dGuo (**1**) and 8-NH₂-Guo (**2**) by N₃[•] Radical (the Dot in the Radicals Are Located on the Atom with Highest Calculated Spin Density)

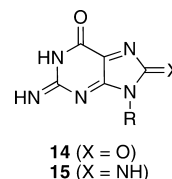
the sharp and intense band at 320 nm and two transitions of moderate intensity at 362 and 382 nm that account for the broad band observed experimentally at 400 nm. On the other hand, the computed absorption spectrum for tautomer **11** is in complete disagreement with the experimental one, since the computed transitions have low intensity and the main transition is computed to occur at a much longer wavelength (443 nm) than in the experimental spectrum. Furthermore, tautomer **10** is more stable than tautomer **11** by 3.8 kcal mol⁻¹ at the PCM/B1B95/6-311+G(2df,p)//B1B95/6-31+G(d,p) level.

Substitution of the oxy group with an amino group at C8 produces only a red shift of the broad band by ~20 nm (at 420 nm, Figure 4). This suggests that, in this case, the two radical species have the same π electronic structure. Indeed, DFT-TD calculations carried out on tautomer **12**, deriving from deprotonation of the amino group at C8 in **2b**, reproduce very well this experimental feature. On the other hand, the computed spectrum for 8-amino tautomer **13**, deriving from deprotonation of **2b** at N1, is in disagreement with the experimental one, since the main band of moderate intensity is computed at 360 nm and the intensity of the band at a longer wavelength (423 nm) is computed to be too low. Furthermore, the imino tautomer **12** is computed to be more stable by 2.3 kcal mol⁻¹ than the amino tautomer **13** at the PCM/B1B95/6-311+G(2df,p)//B1B95/6-31+G(d,p) level.

It is worth mentioning that the spin density (ρ) distribution changes substantially going from radical **10** to radical **12**: in the former ρ is 0.30 on N7 and 0.25 on O8', whereas in the latter ρ is 0.31 on N7 and 0.43 on N8'.³³

γ -Radiolysis coupled with product studies was also carried out with 8-oxo-dGuo (**1**). N₂O saturated solutions containing **1** (1.5 mM) and NaN₃ (12.5 mM) at natural pH (pH 7.2) were irradiated under stationary state conditions with a dose rate of ca. 10 Gy min⁻¹ followed by HPLC analysis. The consumption of **1** led to the formation of several minor products (not identified). The concentrations of **1** decreased as the dose

increases in the range of 0–1.5 kGy, and analysis of the data in terms of radiation chemical yield (G) gives $G(-1) = 0.38 \mu\text{mol J}^{-1}$ when the line is extrapolated to zero dose.³³ Taking into account that $G(N_3^\bullet) + G(H^\bullet) = 0.55 + 0.06 = 0.61 \mu\text{mol J}^{-1}$, ~40% of the starting material is regenerated.³⁵ We suggest that under our experimental conditions the main reaction of radical **10** is the disproportionation to give **1** and **14**, the latter being further transformed to the several minor products either under irradiation or during the workup.¹¹ By replacing 8-oxo-dGuo with 8-NH₂-Guo, similar results were also obtained.



One-Electron Reduced 8-Azidoguanosine (16): An Unexpected Finding. In a parallel pulse radiolysis study of the reaction of hydrated electrons (e_{aq}^-) with 8-N₃-Guo (**16**), we noticed the formation of a single transient whose spectrum shows a remarkable similarity to that of deprotonated one-electron oxidized 8-NH₂-Guo species (Scheme 3). First of all, a rate constant of $1.8 \times 10^{10} \text{ M}^{-1} \text{ s}^{-1}$ was determined for the reaction of e_{aq}^- with **16** at pH ~7.³³ The optical absorption spectrum obtained from the reaction of e_{aq}^- with **16** (blue triangles) is also shown in Figure 4. This is another example of “paradoxical” generation of one-electron oxidized guanine derivatives under reducing conditions, in analogy to the one-electron oxidized guanosine obtained either by oxidation of guanosine or by reduction of 8-bromoguanosine.^{24,25} We suggest that the initial electron adduct is rapidly protonated on the azide moiety to give radical **17** that loses nitrogen, with formation of the observable transient species assigned to radical **12** and/or its tautomeric form **13** (Scheme 3). Based on product studies (see below), also the H[•] atom

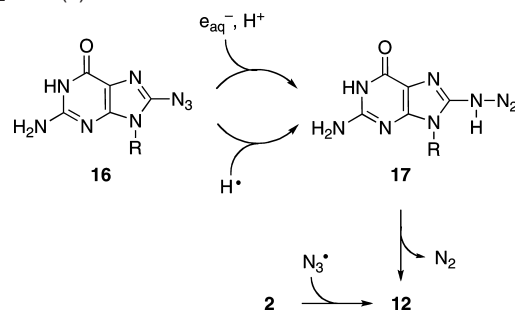
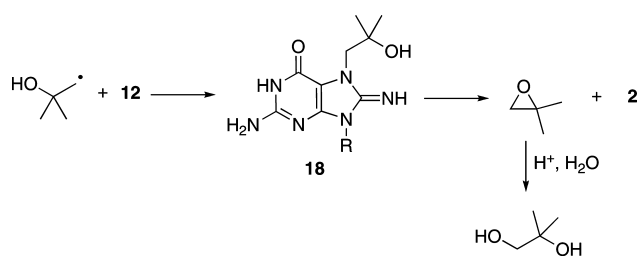
Scheme 3. One-Electron Reduction of 8-N₃-Guo (**16**) Affords **12**, the Same Transient Species of One-Electron Oxidation of 8-NH₂-Guo (**2**)

Table 4. Vertical Optical Transitions (Wavelengths λ , Oscillator Strengths f) for the Tautomers of Deprotonated One-Electron Oxidized 8-NH₂-dGuo Computed at the TD-B3LYP/6-311G(d,p)//B1B95/6-31+G(d,p) Level^a

Tautomers	λ , nm	f	Transition {spin}
12	300	0.190	SOMO ($p\pi(N7) - p\pi(N8')$) $\rightarrow \pi^*(C2-N3) - \pi^*(C6-O6')$ { α }
	370	0.036	SOMO ($p\pi(N7) - p\pi(N8')$) $\rightarrow \pi^*(N1-C2) + \pi^*(C4-N9)$ { α }
	380	0.010	$\pi(C5-N7) - p\pi(N9) - p\pi(O6') \rightarrow$ SOMO ($p\pi(N7) - p\pi(O8')$) { β }
	421	0.065	$p\pi(\text{out-of-phase } N2', N1, O6') \rightarrow$ SOMO ($p\pi(N7) - p\pi(O8')$) { β }
13	283	0.099	SOMO($p\pi(C5) - p\pi(N3) - p\pi(O6')$) $\rightarrow \pi^*(C8-N8')$ { α }
	360	0.082	$p\pi(N7) \rightarrow$ SOMO($p\pi(C5) - p\pi(N3) - p\pi(O6')$) { β }
	388	0.020	$p\pi(\text{out-of-phase } N2', N3, N9, N8') \rightarrow$ SOMO($p\pi(C5) - p\pi(N3) - p\pi(O6')$) { β }
	423	0.013	$p\pi(\text{out-of-phase } N2', N3, N9, N8') \rightarrow$ SOMO($p\pi(C5) - p\pi(N3) - p\pi(O6')$) { β }
	696	0.010	$p\pi(\text{out-of-phase } N2', N1, O6') \rightarrow$ SOMO($p\pi(C5) - p\pi(N3) - p\pi(O6')$) { β }

^a Only transitions with f greater than 0.010 are reported.

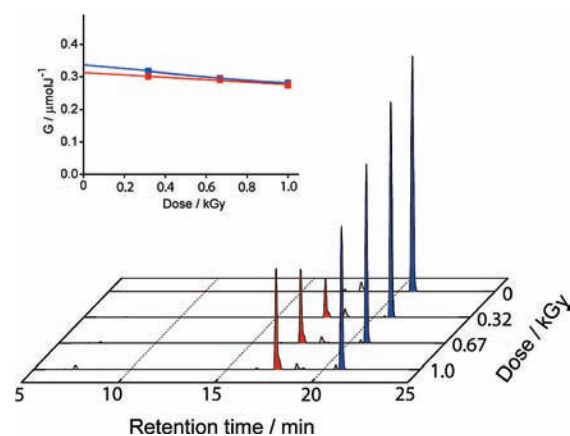
Scheme 4. Proposed Mechanism for the Quantitative Formation of **2** from the Reaction of e_{aq}^- with **16** via Radical **12**

reacted with **16** to potentially afford the same transient species (see below).

Stationary state radiolysis of 8-N₃-Guo (**16**) under reducing conditions was performed. Aqueous solutions of **16** (ca. 1.0 mM) and *t*-BuOH (0.25 M) at pH \sim 7 were prepared. The samples containing 10 mL of deoxygenated solution were irradiated under stationary-state conditions with a dose rate of ca. 10 Gy/min followed by HPLC and LC-MS analysis. The consumption of **16** (blue peaks, Figure 5) led to the formation of a new product, which was determined to be 8-NH₂-Guo **2** (red peaks). The concentrations of **16** and **2** decreased and increased, respectively, as the dose increased in the range of 0–1 kGy. Analysis of the data in terms of radiation chemical yield (G) gives $G(-\mathbf{16}) = 0.33$ and $G(\mathbf{2}) = 0.31 \mu\text{mol J}^{-1}$ when the lines are extrapolated to zero dose (inset, Figure 5).³⁵ Taking into account that $G(e_{aq}^-) + G(H^+) = 0.33 \mu\text{mol J}^{-1}$, our results lead to the conclusion that solvated electrons and hydrogen atoms react quantitatively with **16** to yield **2**.

The effective reduction of 8-N₃-Guo (**16**) to the corresponding 8-NH₂-Guo (**2**) by hydrated electrons deserves a mechanistic consideration.³⁶ Once the intermediate radical **12** is formed (cf. Scheme 3), we suggest that a cross-termination reaction between the nucleoside radical and the $\cdot\text{CH}_2\text{C}(\text{CH}_3)_2\text{OH}$ radical affords adduct **18** (Scheme 4). Adduct **18** can provide **2** upon either hydrolysis and/or intramolecular epoxide ring formation leading to 1,1-dimethyloxirane which subsequently is hydrolyzed to 2-methyl-2,3-propanediol.

To support the proposed mechanism, we tried to identify 1,1-dimethyloxirane in the irradiated mixture. For this purpose, a 1.5 mM solution of 8-N₃-Guo in 5 mL of D₂O containing

**Figure 5.** Irradiation of 8-N₃-Guo **16** (1.0 mM) in the presence of 0.25 M *t*-BuOH at a dose rate of \sim 10 Gy min⁻¹. The HPLC peaks of **16** are highlighted in blue, while the peaks for 8-NH₂-Guo (**2**) are highlighted in red. The inset shows the chemical radiation yields (G) for the consumption of **16** and the production of **2** as a function of the irradiation dose.

t-BuOH (0.25 M) was irradiated with ca. 1.5 kGy, the resulting mixture was lyophilized, and the residue was dissolved in D₂O and analyzed by ¹H NMR.³³ A new peak at 2.65 ppm was observed, which corresponds to the CH₂ protons of the oxirane ring, in accordance with literature data (Scheme 4).³⁷ Unfortunately, due to the overwhelming concentration of *t*-BuOH with respect to that of 1,1-dimethyloxirane, the peaks of the methyl groups could not be observed at 1.30 ppm. Further proof was derived from the acidic hydrolysis of 1,1-dimethyloxirane, which leads to 2-methyl-1,2-propanediol. A drop of DCI was introduced into the NMR tube, and the spectrum obtained after 15 min showed complete conversion of the first to the latter. Indeed, the peak at 2.65 ppm is replaced by a new peak at 3.42 ppm, which corresponds to the hydrogen atoms of the CH₂ group in 2-methyl-1,2-propanediol.^{38,39}

Conclusions

Radical anions of DNA bases have held the interest of chemists for years, and a large body of results exist for nucleosides as simple models.⁴⁰ Our work here demonstrates that the reaction of e_{aq}^- with 8-oxo-dGuo (**1a**) does not lead, after protonation, to transient **3**, an otherwise important intermediate of the hydroxyl radical addition to guanine, but to a

(35) The product yield (mol kg⁻¹) divided by the absorbed dose (1 Gy = 1 J kg⁻¹) gives the radiation chemical yield.

(36) The reduction of **16** to **2** in water by the couple (TMS)₃SiH/HOCH₂CH₂SH under free radical conditions has been recently reported, see: Postigo, A.; Kopsov, S.; Ferreri, C.; Chatgililoglu, C. *Org. Lett.* **2007**, *9*, 5159–5162.

(37) Liu, J.; Houk, K. N.; Dinoui, A.; Fusco, C.; Curci, R. *J. Org. Chem.* **1998**, *63*, 8565–8569.

(38) Cook, G. K.; Mayer, J. M. *J. Am. Chem. Soc.* **1995**, *117*, 7139–7156.

transient species that was characterized as tautomer **5**, through transient spectroscopy and DFT calculations. Contrary to the above system, e_{aq}^- addition to isoelectronic 8-NH₂-Guo (**2b**) leads to a transient species that was characterized as tautomer **7**. Whereas the 8-oxo-dGuo protonated radical anion has the unpaired electron mainly delocalized in the six-membered pyrimidine ring, the 8-NH₂-Guo analogue is mainly delocalized in the imidazolyl ring, accentuating the electronic differences between the two functional groups. On the other hand, the deprotonated one-electron oxidized 8-oxo-dGuo and 8-NH₂-Guo transients were characterized as tautomers **10** and **12**, respectively, clarifying, especially in the case of 8-oxo-dGuo, the ambiguity of previous studies.⁸ In this case, both systems have the unpaired electron density localized in the imidazolyl ring (with the highest calculated spin density residing always on a N). In the case of the 8-NH₂-Guo, the same transient was obtained through e_{aq}^- reaction with 8-N₃-Guo, providing yet another example of generation of one-electron oxidized guanine derivatives under reducing conditions.^{24,25}

Experimental Section

Materials. 8-Oxo-7,8-dihydro-2'-deoxyguanosine was purchased from Berry & Associates and used without any further purification. 8-Aminoguanosine and 8-azidoguanosine were synthesized using standard procedures.^{41,42} All other chemicals and solvents were purchased from commercial suppliers at the highest purity available.

Continuous Radiolysis. Experiments were performed at room temperature (22 ± 2 °C) on 10 mL samples using a ⁶⁰Co-Gammacell, with a dose rate of ca. 10 Gy min⁻¹. The absorbed radiation dose was determined with a Fricke chemical dosimeter, by taking $G(Fe^{3+}) = 1.61 \mu\text{mol J}^{-1}$.⁴³ Reaction mixtures were analyzed by reversed phase HPLC using a Zorbax SB-C18 column (4.6 mm × 150 mm) and eluted in triethylammonium acetate buffer (20 mM, pH 7) with a 0–25% acetonitrile nonlinear gradient over 30 min with a flow rate of 1.0 mL/min (detection at 254 nm). LC/MS analyses were performed with an Agilent 1100 HPLC system and an Esquire 3000 Plus Bruker mass spectrometer using a Zorbax C8 column (4.6 mm × 150 mm, 5 μm) with a 0–25% acetonitrile nonlinear gradient over 30 min at a flow rate of 0.1 mL/min, detection at λ = 254 nm.

Pulse Radiolysis. Pulse radiolysis with optical absorption detection was performed by using a 12 MeV linear accelerator, which delivered 20–200 ns electron pulses with doses between 5 and 50 Gy, by which OH·, H·, and e_{aq}^- are generated with 1–20 μM concentrations.⁴⁴ The pulse irradiations were performed at room temperature (22 ± 2 °C) on samples contained in Spectrosil quartz

cells with a 2 cm optical path length. Solutions were protected from the analyzing light by means of a shutter and appropriate cutoff filters. The bandwidth used throughout the pulse radiolysis experiments was 5 nm. The radiation dose per pulse was monitored by means of a charge collector placed behind the irradiation cell and calibrated with an N₂O-saturated solution containing 0.1 M HCO₂⁻ and 0.5 mM methylviologen, using $G\epsilon = 9.66 \times 10^{-4} \text{ m}^2 \text{ J}^{-1}$ at 602 nm.⁴⁵ $G(X)$ represents the number of moles of species X formed, consumed, or altered per joule of energy absorbed by the system.

Computational Details. Hybrid meta DFT calculations with the B1B95 (Becke88⁴⁶-Becke95⁴⁷ 1-parameter model for thermochemistry) functional⁴⁸ were carried out using the Gaussian 03 system of programs.⁴⁹ This HMDFT model was found to give excellent performance for thermochemistry^{48,50,51} and molecular geometries.^{50,51} An unrestricted wave function was used for radical species. Optimized geometries and total energies were obtained employing the valence double-ζ basis set supplemented with polarization functions and augmented with diffuse functions on heavy atoms (6-31+G(d,p)). The nature of the ground states (zero imaginary frequency) was verified by frequency calculations. Total energies were corrected for the zero-point vibrational energy (ZPVE) computed from frequency calculations using a scaling factor of 0.9735 to account for anharmonicity.⁵⁰ The effect of water solution on the total energies was computed with the polarizable continuum model⁵² (PCM) carrying out calculations at the optimum B1B95/6-31+G(d,p) geometries (PCM(solvent=water)/B1B95/6-311+G(2df,p)/B1B95/6-31+G(d,p)). The time dependent B3LYP method employing a triple-ζ basis set (TD-B3LYP/6-311G(d,p)//B1B95/6-31+G(d,p)) was used to compute optical transitions, since this hybrid DFT method was found by us to provide reliable optical transitions in nucleosides (see text). In Tables 1–4 we have reported the electronic transitions having an oscillator strength f greater than 0.010 and a wavelength λ greater than 280 nm.

Acknowledgment. This research was supported in part by the European Community's Marie Curie Research Training Network under Contract MRTN-CT-2003-505086 (CLUSTOXDNA). The support and sponsorship concerned by COST Action CM0603 on "Free Radicals in Chemical Biology (CHEMBIORADICAL)" are kindly acknowledged. We thank C. Ferreri for many useful discussions and A. Altieri for some preliminary experiments with 8-N₃-Guo. We thank M. Lavalle, A. Monti, and A. Martelli for assistance with the pulse radiolysis experiments.

Supporting Information Available: Product studies, DFT calculations (spin density at the guanine atoms of radicals **4**–**13**, SOMO of radicals **10** and **12**, absolute energies and optimized geometries of calculated structures), pulse radiolysis experiments, and complete ref 49. This material is available free of charge via the Internet at <http://pubs.acs.org>.

JA9065464

- (39) Kinetic support of the mechanism proposed in Scheme 4 can be obtained by analysis of the kinetic decays of radical **12** (insets in Figure 4). The transient **12** obtained from the one-electron oxidation of 8-NH₂-Guo by N₃[·] decays with second-order kinetics (left inset). A value of $k = 2.3 \times 10^8 \text{ M}^{-1} \text{ s}^{-1}$ was obtained as an average from the linear and nonlinear analysis of the trace and associated with the self-disproportionation to give **2** and **15**. On the other hand, the decay of transient **12** generated by the one-electron reduction of 8-N₃-Guo (right inset) corresponds to a larger value of $k = 4.4 \times 10^8 \text{ M}^{-1} \text{ s}^{-1}$, which is associated with the cross-recombination reported in Scheme 4.³³
- (40) von Sonntag, C. *Free-Radical-Induced DNA Damage and Its Repair*; Springer-Verlag: Berlin; 2006.
- (41) Lin, T.-C.; Cheng, J.-C.; Ishiguro, K.; Sartorelli, A. C. *J. Med. Chem.* **1985**, *28*, 1194–1198.
- (42) Saneyoshi, M. *Chem. Pharm. Bull.* **1968**, *16*, 1616–1619.
- (43) Spinks, J. W. T.; Woods, R. J. *An Introduction to Radiation Chemistry*, 3rd ed.; Wiley: New York, 1990; p 100.
- (44) Hutton, A.; G; Roffi, G.; Martelli, A. *Quad. Area Ric. Emilia Romagna* **1974**, *5*, 67–74.

- (45) Mulazzani, Q. G.; D'Angelantonio, M.; Venturi, M.; Hoffman, M. Z.; Rodgers, M. A. *J. Phys. Chem.* **1986**, *90*, 5347–5352.
- (46) Becke, A. D. *Phys. Rev. A* **1988**, *38*, 3098–3100.
- (47) Becke, A. D. *J. Chem. Phys.* **1996**, *104*, 1040–1046.
- (48) Zhao, Y.; Pu, J.; Lynch, B. J.; Truhlar, D. G. *Phys. Chem. Chem. Phys.* **2004**, *6*, 673–676.
- (49) Frisch, M. J. *Gaussian 03, Revision D.02*; Gaussian, Inc.: Wallingford, CT, 2004 (See Supporting Information for the full list of authors).
- (50) Zhao, Y.; Lynch, B. J.; Truhlar, D. G. *J. Phys. Chem. A* **2004**, *108*, 2715–2719.
- (51) Zhao, Y.; Truhlar, D. G. *J. Phys. Chem. A* **2004**, *108*, 6908–6918.
- (52) Tomasi, J.; Menucci, B.; Cancès, E. *THEOCHEM* **1999**, *464*, 211–226.